JOURNAL OF combinatorial CHEMISTRY

Article

Automated Image-Based Method for Laboratory Screening of Coating Libraries for Adhesion of Algae and Bacterial Biofilms

Eraldo Ribeiro, Shane J. Stafslien, Franck Casse#, James A. Callow, Maureen E. Callow, Robert J. Pieper, Justin W. Daniels, James A. Bahr, and Dean C. Webster

J. Comb. Chem., **2008**, 10 (4), 586-594• DOI: 10.1021/cc800047s • Publication Date (Web): 20 June 2008

Algal Adhesion

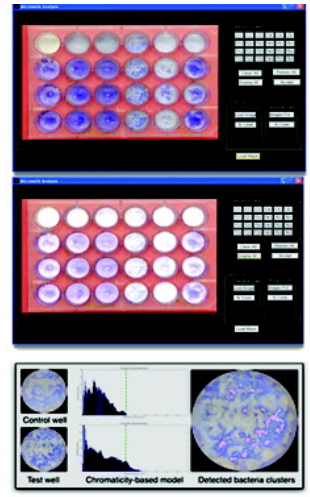

Bacterial Biofilm Adhesion

More About This Article

Additional resources and features associated with this article are available within the HTML version:

- Supporting Information
- Access to high resolution figures
- Links to articles and content related to this article
- Copyright permission to reproduce figures and/or text from this article

View the Full Text HTML

Journal of Combinatorial Chemistry is published by the American Chemical Society. 1155 Sixteenth Street N.W., Washington, DC 20036

Automated Image-Based Method for Laboratory Screening of Coating Libraries for Adhesion of Algae and Bacterial Biofilms

Eraldo Ribeiro,[†] Shane J. Stafslien,*[,‡] Franck Cassé,[§] James A. Callow,[§] Maureen E. Callow,[§] Robert J. Pieper,[‡] Justin W. Daniels,[‡] James A. Bahr,[‡] and Dean C. Webster[‡]

Computer Sciences, Florida Institute of Technology, Melbourne, Florida 32901, Center for Nanoscale Science and Engineering, North Dakota State University, Fargo, North Dakota 58102, and School of Biosciences, The University of Birmingham, Birmingham B15 2TT, U.K.

Received March 20, 2008

Assessment and down-selection of non-biocidal coatings that prevent the adhesion of fouling organisms in the marine environment requires a hierarchy of laboratory methods to reduce the number of experimental coatings for field testing. Automated image-based methods are described that facilitate rapid, quantitative biological screening of coatings generated through combinatorial polymer chemistry. Algorithms are described that measure the coverage of bacterial and algal biofilms on coatings prepared in 24-well plates and on array panels, respectively. The data are used to calculate adhesion strength of organisms on experimental coatings. The results complement a number of physical and mechanical methods developed to screen large numbers of samples.

Introduction

The majority of antifouling coatings in current use are based on biocides, such as copper,[1] and organic compounds that readily degrade once released from the paint.[2] Increasing environmental concerns and escalating costs of registration and regulatory compliance have resulted in the need to find alternative environmentally benign technologies to control biofouling.[3,4] Non-biocidal coatings, the so-called fouling-release coatings exemplified by silicone elastomers, are not inherently antifouling but, organisms attach only weakly and therefore are released by hydrodynamic forces like those experienced by a fast moving boat.[5] Screening the antifouling potential of biocidal antifouling paints is relatively straightforward. New formulations are typically painted onto large panels that are hung from rafts, and the presence of different types of fouling organisms is scored over time. Non-biocidal formulations necessitate more complex methods of assessment, and laboratory evaluations are frequently employed to aid down-selection of formulations for field testing. Because the settlement of fouling organisms is rarely inhibited on non-toxic coatings, a measure of the relative adhesion strength of the attached organisms is required. Moreover, because different fouling organisms appear to adhere to different degrees,[6,7] a number of test organisms need to be employed.

North Dakota State University has developed a high-throughput capability to produce novel environmentally benign coatings for the marine environment.[8–10] Because the number of formulations generated from one concept could be as many as several hundred, down-selection on the basis of laboratory assays is essential. Typically, the first down-selection is based on various surface and mechanical tests,[8,10] followed by a second down-selection based on a number of biological assays.[11–15] Coatings can be deposited in a range of formats for subsequent evaluation including 24-well plates[11–15] and array panels.[16]

This paper reports methods to quantify biofilm coverage on coating surfaces using new algorithms that allow quantification of a large number of samples. The biofilm quantification methods presented in this paper are based on Gaussian mixture−model color segmentation techniques. The technique was successfully applied to two main types of biofilm quantification. The first was the detection of retracted bacterial biofilm on coatings cast in 24-well plates. The second was the quantification of algal biomass on 12-patch array panels. Quantification results obtained in this study are promising and demonstrate the effectiveness of the automated biofilm quantification methodology.

Two groups of organisms, namely, bacteria and algae were employed in two formats, namely, 24-well plates and array panels, respectively. Bacterial biofilm coverage on coatings deposited in wells of 24-well plates was quantified after drying and staining. Coverage of patches of coatings deposited in groups of 12 on array plates was determined after a lawn of young plants of the green macroalga *Ulva* cultured on the array panels was sprayed at specific impact pressures by a water jet. The set of coatings used to demonstrate the methods was a group of 24 siloxane-acrylic-polyurethane coatings.[17]

The marine bacterium *Cellulophaga lytica* (formerly *Cytophaga lytica*) was used to evaluate microbial biofilm

* To whom correspondence should be addressed. Phone: 701-231-5826. Fax: 701-231-7916. E-mail: Shane.Stafslien@ndsu.edu.
[†] Florida Institute of Technology.
[‡] North Dakota State University.
[§] The University of Birmingham.

10.1021/cc800047s CCC: $40.75
Published on Web 06/20/2008

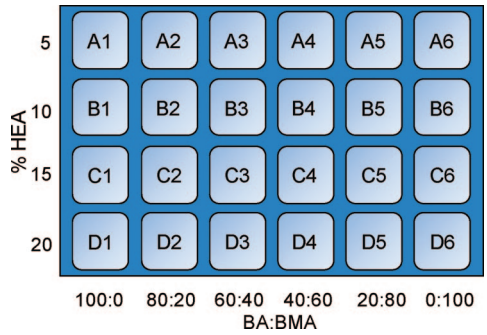

Figure 1. Experimental design of combinatorial acrylic polyol library.

adhesion to the siloxane-polyurethane coating surfaces.[13] Measurement of the strength of attachment of young plants (sporelings) of the green macroalga *Ulva* to surfaces provides an indication of the fouling-release properties of higher fouling organisms.[18–21]

Experimental Section

Coating Library Synthesis. The preparation of the siloxane-acrylic-polyurethane coating library has been reported in detail elsewhere.[17] Briefly, a library of 24 acrylic polyols was synthesized by solution free radical polymerization. The monomers consisted of hydroxyl ethyl acrylate, which was varied from 5 to 20 wt %, and butyl acrylate and butyl methacrylate, which were varied systematically from a ratio of 0:100 to 100:0. The experimental design is shown in Figure 1. The acrylic polyols were then incorporated into a siloxane-acrylic-polyurethane coating formulation consisting of 10% of a 3-aminopropyl-terminated PDMS (10,000 g/mol)[22] and an isocyanate cross-linker (Tolonate HDT from Rhodia). The ratio of isocyanate to amine + hydroxyl functional groups was 1.1:1.0. The formulation also consisted of 2,4-pentanedione as a pot life extender, dibutyl tin diacetate as cure catalyst, and solvents toluene, methyl amyl ketone, and ethyl ethoxy propionate. Control silicone elastomers DC 3140 and T2 Silastic were received from Ellsworth Adhesives. DC 3140 and T2 Silastic were solvent reduced with MIBK and called silicone A and silicone B, respectively.

Coating Application and Curing. For bacterial analysis, the siloxane-urethane coatings were solvent cast into modified 24-well polystyrene plates as described previously.[11] Each unique coating formulation was deposited into one column of a 24-well plate, providing four coating replicates for analysis. The first column of each array plate contained the standard siloxane coating A.

A Symyx Coating Application system was used to apply formulations to 4 × 8 in. aluminum panels for algal analysis;[8] 0.1 mL of each coating formulation was deposited on the panels using disposable pipettes to prevent cross contamination, and then a robotic doctor blade spread the coating at a wet film thickness of 200 μm. The automated doctor blade was washed with toluene under sonication three times after each application and dried with an air knife. After completion of deposition of all the coatings, the panels were removed from the coating application station, placed into an enclosed drying cabinet with ventilation, and left overnight to cure at ambient temperature. Coatings were cured at 100 °C for one hour the following day.

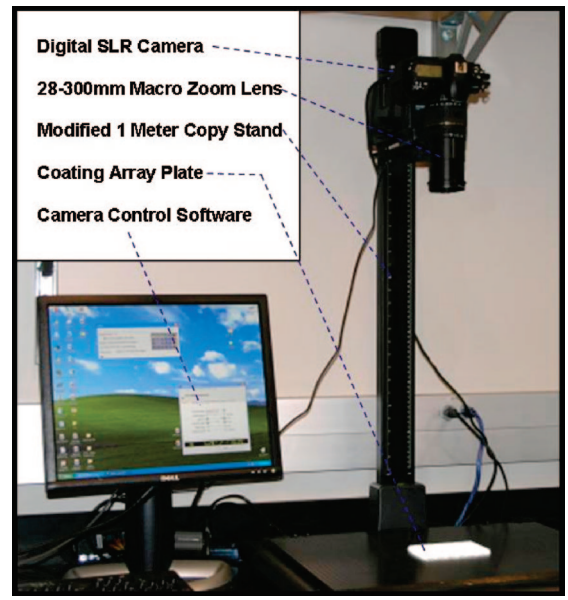

Figure 2. Digital imaging station used to capture high resolution photographs of 24-well coating array plates.

Bacterial Bioassay. The measure of bacterial biofilm adhesion to the siloxane-urethane coating surfaces was determined by using a high-throughput bacterial biofilm retention and retraction assay.[13] An overnight culture of the marine bacterium *Cellulophaga lytica* (formerly *Cytophaga lytica*) was resuspended in sterile artificial seawater supplemented with nutrients ($\sim 10^7$ cells ml^{-1}). Rows 2−4 were inoculated with 1 mL of the *C. lytica* suspension, while row 1 received nutrient medium only. The coating array plates were incubated statically for 18 h at 28 °C in a temperature controlled water bath. After 18 h of incubation, the array plates were rinsed three times with deionized water and dried for ∼1 h at ambient conditions. The array plates were then stained with a biomass indicator dye, crystal violet (CV), for 15 min, and rinsed three times with deionized water to remove excess CV.

High-resolution images of the CV-stained coating array plates were acquired with a Nikon D200 digital single lens reflex camera set at 10 megapixels per image. The camera was permanently mounted to a modified 1 m high copy stand and controlled by Nikon Camera Control Pro software to provide a stable hands-off configuration (Figure 2). A Tamron 28−300 mm macrozoom lens was used to capture the entire array plate in a single image and at a distance sufficient enough to minimize obstruction from the well walls. Array plates were loaded into the recess on the copy stand deck and images were collected through the software.

After digital images of each array plate were taken, CV was extracted from the biofilm retained on the coating surfaces by addition of 0.5 mL of 33% glacial acetic acid.[11] 0.15 mL of the resulting eluates were transferred to a 96-well plate and measured for absorbance at 600 nm with a multiwell plate reader. The absorbance value reported for each siloxane-urethane coating was the mean value of three replicate wells. Error bars represent one standard deviation of the mean.

Algal Bioassay. Zoospores were obtained from fertile *Ulva linza* plants as described in Callow et al.,[23] and the spore concentration was adjusted to 1×10^6 spores ml^{-1}. Three replicates of each of the three array panels were incubated in trays (three plates in each tray) of 30.5 × 21 cm with 300 mL of zoospore suspension for 3 h in darkness at ~20 °C. During this time, a proportion of the total number of spores settled, that is, adhered to the surface panels. Unattached (swimming) spores were removed by washing the plates gently in artificial seawater.

The panels were transferred to glass tanks (19 × 20 × 60 cm) containing 10 L of 10% strength enriched seawater medium.[24] Three plates were incubated in each of three tanks, and the position of the plates was changed daily. Each tank was fitted with a pump that recirculated the medium inside the tank at 200 L h^{-1}. Illumination was provided by two daylight fluorescent tubes placed above the tank (Boyu PL-18 W) that provided an irradiance of 32 μmol m^{-2} s^{-1}. After 5 days, the spores had germinated, and the sporelings (young plants) formed a green mat over the surface of the plates (Figure 3).

Each set of three plates was exposed to an automated water jet at a different uniform surface pressure. The water jet[25] was programmed to raster six times across the middle of each of the three rows of samples. The surface impact pressures used were 93, 151, and 171 kPa. Photographs were taken of each plate before and after jet washing using a digital camera (Sony DSC-S75) set at 1.8 Mega Pixels.

Image Segmentation for Biofilm Retraction Quantification. The biofilm quantification algorithm described in this section uses a color segmentation method based on a Gaussian mixture model.[26] In this model, the color of biofilm pixels is represented by probability distributions. The work in this paper describes two applications of the procedure. The first of these is the detection of retracted bacterial biofilm on coatings cast in 24-well plates. The second is the quantification of algal biomass on 12-patch array panels.

The goal of the algorithm is to classify all image pixels according to their estimated color models. The result of this classification procedure is an image segmented into two distinct regions: biofilm regions and non-biofilm regions. Once these regions are at hand, quantifications such as percent biofilm surface coverage estimation can be obtained by means of a straightforward frequency count of the labeled pixels.

Modeling Biofilm Color Distributions. The key assumption of the method is pixel color is a realization of a multimodal distribution of color segments. This multimodal distribution can be represented by a Gaussian mixture model[26] of K components given by

$$p(x|\Theta) = \sum_{i=1}^{k} \alpha_i p_i(\mathbf{x}|\theta_i) \tag{1}$$

where $\mathbf{x}$ is a color vector,α_i represents the mixing weights such that $\Sigma_{i=1}^{k}\alpha_i = 1$, Θ represents the collection of parameters (α_1,..., α_K, θ_i,..., θ_K) with $\theta = (\mu, \Sigma)$, and p_i is a multivariate Gaussian density function as given by

$$\rho(\mathbf{x}_i|\, j) = \frac{1}{2\pi|\sum_j|^{1/2}} \exp\left\{-\frac{1}{2}(\mathbf{x}_i - \mu_j)^{\mathbf{T}} \sum_j^{-1} (\mathbf{x}_i - \mu_j)\right\} \tag{2}$$

where $\mathbf{x}_i = [H,S]^{\mathbf{T}}$ is the color of the i-th pixel in the image, μ_j represents the two-dimensional mean vector of the j color segment, and Σ_j its 2 × 2 covariance matrix. $|\Sigma_j|$ is the determinant of Σ_j. In this paper, images are represented using the HSV (hue, saturation, and value) intensity decoupling color model.[27] The color of each image pixel is represented by a vector formed by the hue and saturation components in the HSV model (i.e., chromaticity components). Neglecting the relative luminance component V helps reduce the algorithm's sensitivity to small illumination variations.

Biofilm segmentation is accomplished by estimation of the parameters of the densities describing the image's color populations (eq 1). The final pixel labeling procedure consists of determining the color segment model with the maximum likelihood for each image pixel. Each component of the Gaussian mixture represents a color segment in the image. If $\mathbf{x}$ is assumed to be sampled independently from $p(\mathbf{x})$, then the probability of the whole image is given by

$$\mathscr{L}(\Theta) = \prod_{i=1}^{K} p(\mathbf{x}|\Theta) = \prod_{i=1}^{N} \sum_{j=1}^{k} \alpha_j p(\mathbf{x}|\, j) \tag{3}$$

In general, there are two ways to obtain the parameters of the above density functions. If prior information about the labeling of pixels belonging to the biofilm and non-biofilm classes is available, the density estimation is called *supervised*. In this case, it is assumed that the user is able to provide a selection of regions containing only biofilm pixels, as well as a region containing only non-biofilm pixels. Once these regions are at hand, the estimates of the mean vector and the covariance matrix in eq 2 for each color population are given by

$$\hat{\mu}_j = \frac{1}{N}\sum_{i=1}^{N} \mathbf{x}_i$$

and

$$\hat{\Sigma}_j = \frac{1}{N}\sum_{i=1}^{N} (\mathbf{x}_i - \hat{\mu}_j)(\mathbf{x}_i - \hat{\mu}_j)^{\mathbf{T}} \tag{4}$$

where N is the total number of pixels in the selected image region. On the other hand, if no labeling information is available, the estimation is said to be *unsupervised*. Unsupervised classification allows for reduced interaction and fully automated segmentation methods. In this case, the input to the segmentation algorithm is simply the image to be segmented. The algorithm must estimate pixel membership and density parameters simultaneously by maximizing eq 3 with respect to the model parameters. This maximization problem is solved using the expectation−maximization (EM) algorithm.[28] In the segmentation method proposed in this paper, a K-means algorithm[29] is used to obtain the initial values for the unknown mean vectors μ_1,..., μ_k. The initial covariance matrices Σ_1,..., Σ_k are chosen to be the identity matrices.

Detecting Retracted Biofilm Regions. Digital images of the coating array plates were loaded into the graphical user interface (GUI) of the percent coverage software program. A mask was then generated and applied to the loaded image (Figure 4). The percent biofilm coverage for each well of the

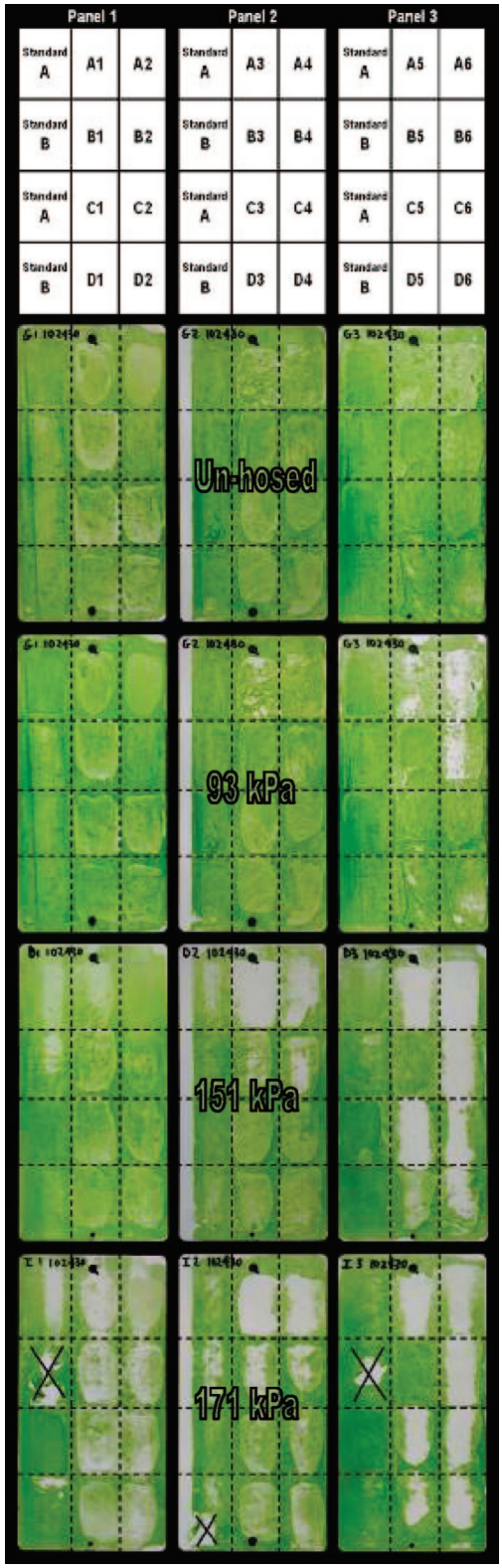

Figure 3. Biomass of *Ulva* sporelings on array panels after 5 days growth and after being sprayed with a hose at three different impact pressures. The top row shows the configuration and codes of the 36 paint patches (24 novel formulations) on the three array panels. Two patches of two standard siloxanes (standard A and B) are represented on the left-hand side of every panel. The first row of images shows a set of three panels before spraying. The second, third, and fourth row of images shows sets of panels after hosing at 93, 151, and 171 kPa of impact pressure, respectively. The panels sprayed at 93 kPa were those shown before they were sprayed (top row of images). The black crosses indicate coating failure hence these patches were excluded from the analysis.

plate was determined and exported to Microsoft Excel by executing the software. The percent coverage value for each coating was reported as the mean value of three replicate wells. Error bars represent one standard deviation of the mean.

The concentration of the crystal violet staining color on the coating surfaces is the main discriminative visual information used for the detection of bacterial biofilm. Traditionally, bacterial biofilm detection is achieved by visually distinguishing test well regions in which the staining color appears distinctively darker than regions in corresponding control wells. Color variations in the control wells results from the crystal violet dye binding or interacting with the coating material itself. The actual color distribution on the coating surfaces is found to be multimodal, having at least three main dominant components. The first component is the bright color of the clean background. This color is usually the most frequent in the control wells. It is also present in regions from which the bacterial biofilm has retracted on the coating surface. The second color segment is the retracted bacterial biofilm represented by the crystal violet dye used in the experiments. Nevertheless, some of the violet dye might also appear in the control wells. In this case, it appears in significantly low frequencies. The third color segment consists of noisy pixel colors originated from illumination artifacts such as reflections and specularities.

The biofilm segmentation method estimates the parameters of this three-mode color pattern distribution in the multiwell plates using the EM algorithm[28] as described previously. This procedure is performed separately for each well in the plate. The majority of pixels in the control wells should belong to the background color class. This information is used to determine the label of the background color segment. The other two labels are easily determined by using the strong blue component of the violet dye as a disambiguating clue. At the end of this step, the labeled model densities and prior distributions represent the colors for the biofilm, background, and noise regions, respectively.

However, the sporadic presence of violet color pigmentation creates the need for a further comparison of the distributions of the labeled biofilm components. Here, the focus in on the violet color density only. This additional step is performed to determine a threshold indicating the main difference between violet color distributions in the control well and the one in the corresponding test wells. This procedure is performed separately for each column of the multiwell plate (i.e., a set of corresponding control and test wells).

To obtain a simple threshold value, a combined chromaticity map of the biofilm pixels is created. This map is given by $\mathbf{y}(i) = \mathbf{h}(i) \times \mathbf{s}(i)$ and allows for a one-dimensional distribution of the violet color with values ranging from brighter to darker violet. Consequently, the value of the segmentation threshold for of the settled biofilm with respect to a given control well can be set to the maximum value of the combined chromaticity map, that is, $\mathbf{T} = \max_i \mathbf{y}_c(i)$, where $\mathbf{y}_c(i)$ is the combined chromaticity map of the biofilm color component in the corresponding test well. The retracted biofilm pixel map is then given by

$$\mathbf{b}_r(i) = \begin{cases} 1 & \text{if } \mathbf{y}_t(i) \geq \boldsymbol{T} \\ 0 & \text{otherwise} \end{cases} \quad (5)$$

Here, $\mathbf{y}_t(i)$ is the combined chromaticity map of the biofilm color component in the control well. Finally, the calculation of percent cover is given by $p_t = (100/N)\sum_i \mathbf{b}_r(i)$, where N is the total number of pixels in the region of interest in the test well image. Algorithm 1 summarizes the main steps of the process (Figure 5A).

Quantifying Biomass of *Ulva*. Quantification of biomass of the green alga *Ulva* is another application of the color segmentation methods described in this paper. The biofilm's dominant color is green instead of violet. In addition, the segmentation problem is mostly a binary one. The goal of the quantification is to determine the area percentage of the high-pressure water jet removed algae on the test panels. The supervised segmentation approach is used in this case. The user provides two selected image subregions as input to the program. The two image subregions contain pixels from algae and non-algae regions, respectively. The program estimates the density parameters of each pixel color population using the equations in 4. The resulting labeling of algal pixels is accomplished by a maximum likelihood classification. The percent of remaining algal biomass is calculated as described previously in this paper.

Another important part of the method to quantify algal biomass is the perspective distortion removal step. This step allows for the alignment of *Ulva* panels that present perspective distortion because of the angle at which the images are acquired (Figure 6). The rectification step helps ensure the repeatability of the experiments. The details of

Figure 4. Coating array plate image loaded into the graphical user interface (top). Mask applied to the plate image (bottom). White regions of the mask show the precise area used to calculate percent surface coverage for each well of the coating array plate.

(A)

Algorithm 1 Detection of retracted biofilm regions

1: Extract all subregions of interest inside the microwells.
2: $K \leftarrow 3$ (Equation 1)
3: **for** every microwell subregion **do**
4: Estimate $\hat{\Theta} = \arg\max_{\Theta} \mathcal{L}(\Theta)$ using E.M algorithm.
5: **for** every pixel **do**
6: Obtain pixel labels (biofilm, background, noise).
7: **end for**
8: **end for**

(B)

Algorithm 2 Ulva settlement quantification

1: Register all panel images using $\mathbf{x} = H\mathbf{x}$.
2: Select biofilm image region.
3: Select non-biofilm image region.
4: Calculate densities $p(\mathbf{x}_i|\text{Ulva})$ and $p(\mathbf{x}_i|\text{Background})$ using Eqs. (2) and (4).
5: **for** every pixel in the panel image **do**
6: Obtain ML pixel labels (biofilm, background).
7: **end for**
8: Calculate biofilm percent cover for selected regions of interest.

Figure 5. Software algorithm used to quantify (A) bacterial biofilm and (B) algal percent surface coverage on multiwell coating plates and coating array panels, respectively.

the planar rectification process[30] is summarized as follows. The perspective distortion observed for the *Ulva* panel images corresponds to a plane-to-plane transformation and can be represented by a 3 × 3 planar projective transformation, H, also called planar homography. Under planar homography, image points are mapped as

$$\mathbf{x} = H\mathbf{x}' \tag{6}$$

where $\mathbf{x}$ and $\mathbf{x}'$ are represented in homogeneous coordinates. Pixel coordinates in the distorted images are represented by $\mathbf{x} = (x, y, 1)^{\mathbf{T}}$. Pixel coordinates in the undistorted (i.e., rectified) image are given by $\mathbf{x} = (x_1, x_2, x_3)^{\mathbf{T}}$. Here, we focus on the case of planar projective transformation. The geometric transformation has 8 degrees of freedom. The image points $\mathbf{x}$ and $\mathbf{x}'$ correspond to the same point X in the world. To solve for the transformation H, we need at least four pairs of corresponding points in the images. In our current implementation, the user manually selects these points using the mouse. Once the four pairs of points are determined, the algorithm estimates the transformation H and rectifies the panel images to a fronto-parallel view using the homography mapping in eq 5. Algorithm 2 summarizes the main steps of the process (Figure 5B).

Results

Twenty-four-Well Plate Evaluations. Figure 7shows the images of the coating array plates after crystal violet staining. A large variation in the degree of surface coverage of retained *C. lytica* biofilm on the siloxane-polyurethane coatings was observed. To facilitate direct comparison, a representative image of each coating is also shown in Figure 7. The data in Figure 8A and B illustrates two methods of analysis of the biofilm on the test coatings. Figure 8A shows total biomass quantified following extraction of crystal violet. In general, the amount of retained biomass was similar throughout the siloxane-polyurethane coating library. The percent coverage measurements for each experimental coating using the automated software program are shown in Figure 8B. Several coatings exhibited a high degree of biofilm retraction (i.e., low surface coverage) indicating reduced *C. lytica* biofilm adhesion to those surfaces.[13] Examination of the coating array plate images shows that a significant amount of crystal violet dye bound to three of the experimental siloxane-polyurethane compositions (B6, C6, and D6) (Figure 7). In the case of coating D6, the binding of crystal violet dye did not significantly interfere with the percent coverage analysis as the biofilm retraction was moderate on this surface. However, a high degree of biofilm retraction was observed on coatings B6 and C6. The dense areas of retracted biofilm on these coating surfaces were adequately detected by the chromaticity threshold determination method described above (Figure 9).

Twelve-Patch Array Panel Evaluations. There was a complete coverage of algal sporelings over all nine panels after 5 days growth (only one set is shown in Figure 3). Each set of panels was exposed to a different surface impact pressure by hosing with a calibrated water jet. The sets of panels after they were sprayed at 93, 151, and 171 kPa, respectively, are shown in Figure 3. It can be seen that different formulations release the algal biomass growing on the surface more effectively than others. Figure 3 also shows that biomass removal increases with increasing impact pressure.

The percent coverage of biomass (green color) on every patch was quantified using the software described above. Figure 10A shows percent removal at the three impact pressures for five formulations, chosen to represent the range of fouling release performance from good to bad. From such plots, the critical impact pressure for removal of 50% coverage of biomass can be determined. Figure 10B shows the experimental formulations in terms of critical pressure. Six experimental coatings coatings (A2, B5, C3, C4, D1, D3) and standards A and B are excluded from the plot because 50% removal was not achieved at the highest impact pressure used.

Discussion

Large numbers of experimental coatings can be generated very quickly using a combinatorial, high-throughput ap-

Figure 6. Illustration of the image analysis program that calculates percentage coverage of *Ulva* sporelings on the panels. The image shows panel 2 after it was sprayed at 151 kPa of impact pressure. The zone of interest has been selected on patch B4, followed by the foreground and background. The percent cover calculation highlights the green biomass inside the zone of interest and therefore provides the percentage cover inside the selected area.

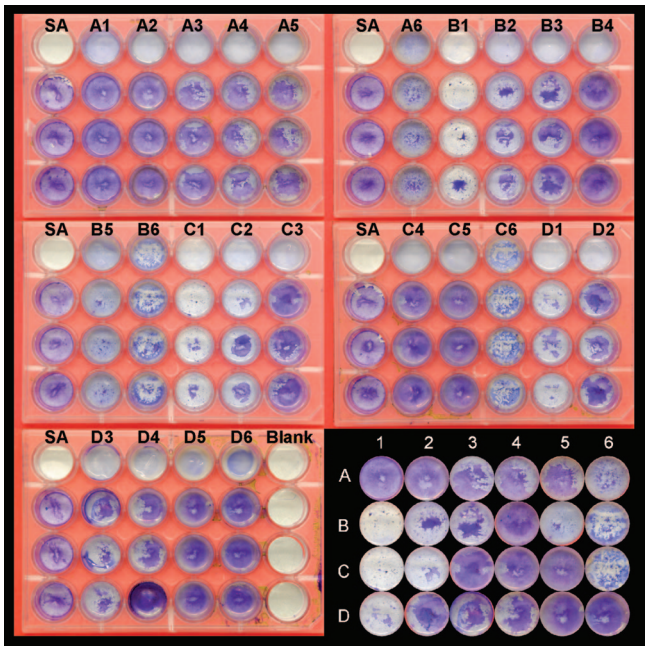

Figure 7. *C. lytica* biofilm surface coverage on the siloxane-urethane coatings after staining with crystal violet. The first column of each array plate contained standard siloxane A (SA). Columns 2−6 contained experimental siloxane-urethane coatings. The top row of each array plate was inoculated with nutrient medium only. Rows 2−4 were inoculated with a nutrient medium suspension of *C. lytica*, providing three replicate samples for analysis. The bottom right image shows a representative well for each of the 24 unique siloxane-urethane coating compositions.

proach.[31] This necessitates the development of automated toolsets and assays to quickly screen coating libraries for various properties and identify promising compositions that may warrant further investigation. In the case of antifouling marine coatings development, one of the primary performance screens is typically a biological laboratory assay. These assays use one or more array formats (i.e., 24-well plates, 12-patch panels) that allow for rapid and efficient analysis of experimental coatings in parallel.

The high-throughput biological screening methods developed to date use a variety of spectrophotometric and imaging methods to quantify the biomass of marine organisms biomass on the surface of coating arrays. Although effective, the imaging methods employed are tedious, time-consuming, and require manual manipulation and analysis of each coating image by the investigator. This includes the determination of percent surface coverage of the marine organism for measurement of adhesion strength on fouling-release coatings.[13,16]

We have reported here on the development of an automated imaging software tool to quantify bacterial and algal percent coverage on coating arrays. It is important to emphasize that biofilm coverage of the coating surface and not total biomass is being quantified by the algorithms described here. The difference is shown clearly for the bacterial data, where extraction of dye revealed only small differences between the samples (Figure 8A) compared to quantification of the area of surface covered by biofilm (Figure 8B). A measure of surface coverage is the more relevant parameter when down-selecting coatings on the basis of their fouling release potential.

The accuracy of analysis is greatly improved by the imaging software as an algorithm is consistently applied to each coating image, rather than a subjective calculation made by the investigator. In addition, the throughput of coating analysis is

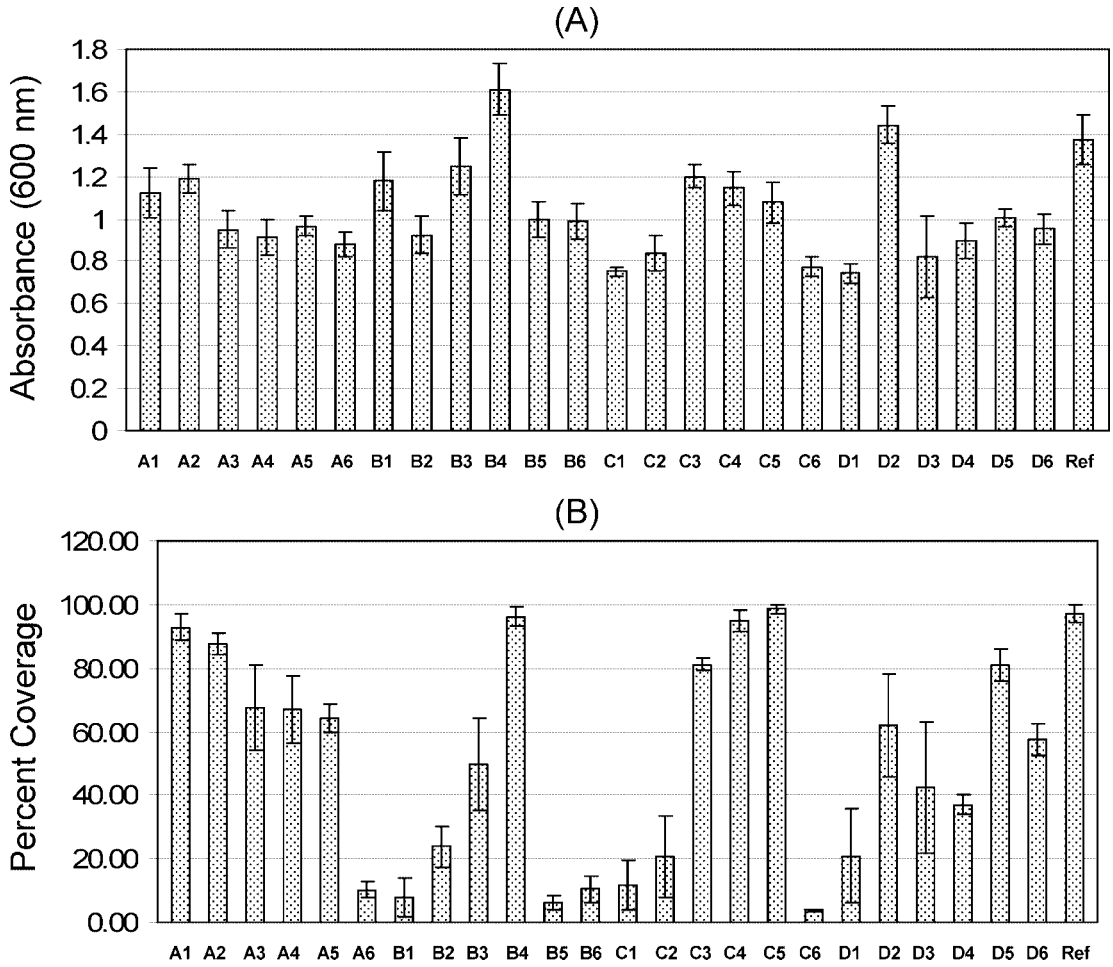

Figure 8. Assessment of *C. lytica* biofilm retention and retraction on the siloxane-urethane coatings using the HTBRRA. (A) *C. lytica* biofilm retention as determined by absorbance measurements (600 nm) of crystal violet extractions in 33% glacial acetic acid. (B) *C. lytica* biofilm retraction as determined by percent surface coverage measurements obtained from digital images of crystal violet stained coating array plates. Each data point was reported as the mean value of three replicate coating samples. Error bars represent one standard deviation of the mean.

significantly enhanced because each coating of an array plate is analyzed simultaneously by the software program and exported to a common database. As many as 200−300 patches on array panels or 24-well plates can be analyzed in one experiment (180−360 experimental patches/wells). The limiting factor in the number of coating arrays that can be analyzed in one experiment is the amount of time needed for plate processing (i.e., rinsing, staining, and water jetting, etc.), rather than the time needed to process the images. The only requirement is that good quality digital images of the coating array plates are obtained for accurate and efficient analysis. In certain instances, reflected light may be captured on the coating surface during the imaging process and compromise the ability of the imaging software to adequately quantify percent coverage. This phenomenon can potentially be avoided by the use of an appropriate lighting tent.

The ultimate goal of the automated imaging software tool is to aid in the rapid and accurate identification of promising coatings compositions from large numbers of candidate materials. Because there are many species of marine organisms responsible for fouling, it is important that the primary biological laboratory screening assays include more than one particular organism to appropriately down-select coatings.

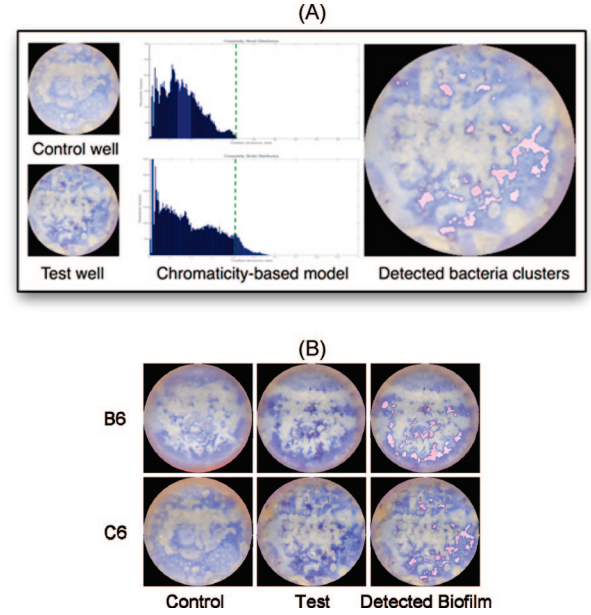

Figure 9. (A) HSV-based color distribution models for a siloxane-urethane control and test well. Color distribution models are used to accurately discriminate between crystal violet stained biofilm (test well) and crystal violet stained coating surface (control well). (B) Images of control wells, test wells, and detected regions of retracted biofilm for siloxane-urethane compositions B6 and C6.

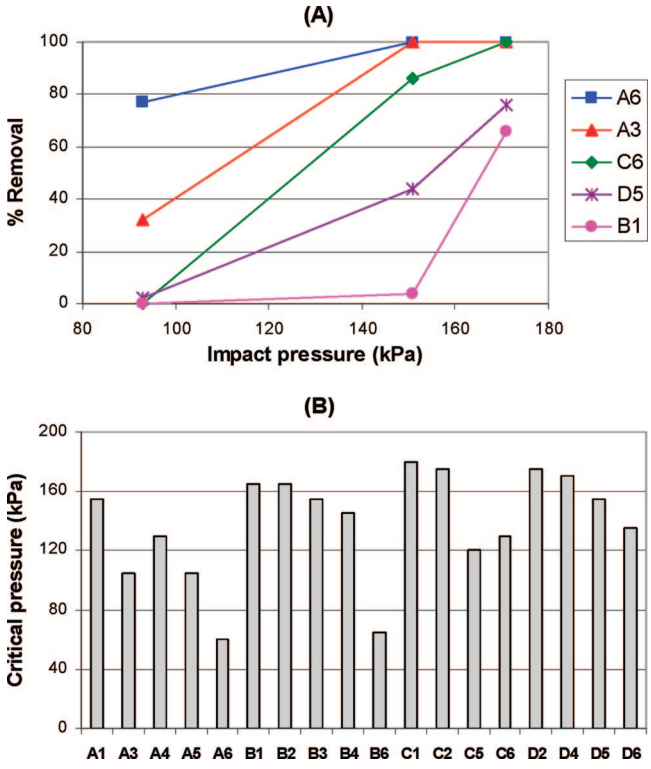

Figure 10. Fouling release performance as assessed by the ease of removal of *Ulva* sporelings. (A) Five patches (A3, A6, B1, C6, and D5) were selected out of 24 experimental coatings to illustrate the range of release performance at three different impact pressures. (B) Plot showing the impact pressure required to achieve 50% removal (critical pressure) from each coating surface. Coatings A2, B5, C3, C4, D1, D3 and standards A and B are not included because less than 50% biomass was removed at the highest pressure.

As shown in Figure 10B, analysis of the coatings with *Ulva* indicates that two coatings, A6 and B6, had superior fouling release performance (i.e., lowest critical removal pressure). These two coatings also exhibited a low bacterial biofilm surface coverage (i.e., high degree of biofilm retraction). However, several other coatings that showed a high degree of biofilm retraction (B1, B5, C1, C2, and C6) performed quite poorly in terms of the release of *Ulva* biofilm. If the amount of coating material, labor, or cost of testing, etc., is not a limiting factor, all coatings that performed well in both assays could be scaled up for ocean testing. In reality, the data from these two bioassays would be considered alongside adhesion data for pseudobarnacles,[32] diatoms (i.e., slime forming unicellular algae),[15] and barnacle adhesion.[33] Thus, the 200−300 coating formulations evaluated with bacteria and algae would typically be reduced to approximately 10 for full ocean testing.

Acknowledgment. Financial support from the Office of Naval Research through ONR Grants N00014-05-1-0822 and N00014-06-1-0952 is gratefully acknowledged.

References and Notes

(1) Finnie, A. A. *Biofouling* **2006**, *22*, 279–291.
(2) Turley, P. A.; Fenn, R. J.; Ritter, J. C.; Callow, M. E. *Biofouling* **2005**, *21*, 31–40.
(3) Swain, G. E. *Paint Coat Eur.* **1999**, 18–25.
(4) Genzer, J.; Efimenko, K. *Biofouling* **2006**, *22*, 339–360.
(5) Kavanagh, C. J.; Quinn, R. D.; Swain, G. W. *J. Adhes.* **2005**, *81*, 843–868.
(6) Holland, R.; Dugdale, T. M.; Wetherbee, R.; Brennan, A. B.; Finlay, J. A.; Callow, J. A.; Callow, M. E. *Biofouling* **2004**, *20*, 323–329.
(7) Holm, E. R.; Kavanagh, C. J.; Meyer, A. E.; Wiebe, D.; Nedved, B. T.; Wendt, D.; Smith, C. M.; Hadfield, M. G.; Swain, G.; Darkangelo, C.; Truby, K.; Stein, J.; Montemarano, J. *Biofouling* **2006**, *22*, 233–243.
(8) Webster, D.; Bennett, J.; Keubler, S.; Kossuth, M.; Jonasdottir, S. *JCT Coat. Technol.* **2004**, *1*, 35–39.
(9) Webster, D. C.; Chisholm, B. J.; Stafslien, S. J. *Biofouling* **2007**, *23*, 179–192.
(10) Chisholm, B. J.; Webster, D. C.; Bennett, J. C.; Berry, M.; Christianson, D.; Kim, J.; Mayo, B.; Gubbins, N. *Rev. Sci. Instrum.* **2007**, 78.
(11) Stafslien, S. J.; Bahr, J. A.; Feser, J. M.; Weisz, J. C.; Chisholm, B. J.; Ready, T. E.; Boudjouk, P. *J. Comb. Chem.* **2006**, *8*, 156–162.
(12) Stafslien, S.; Daniels, J.; Chisholm, B.; Christainson. D. *Biofouling* **2007**, *23*, 37–44.
(13) Stafslien, S.; Daniels, J.; Mayo, B.; Christianson, D.; Chisholm, B.; Ekin, A.; Webster, D.; Swain, G. *Biofouling* **2007**, *23*, 45–54.
(14) Stafslien, S. J.; Bahr, J. A.; Daniels, J. W.; Vander Wal, L.; Nevins, J.; Smith, J.; Schiele, K.; Chisholm, B. *Rev. Sci. Instrum.* **2007**, 78.
(15) Cassé, F.; Stafslien, S. J.; Bahr, J. A.; Daniels, J.; Finlay, J. A.; Callow, J. A.; Callow, M. E. *Biofouling* **2007**, *23*, 121–130.
(16) Cassé, F.; Ribeiro, E.; Ekin, A.; Webster, D. C.; Callow, J. A.; Callow, M. E. *Biofouling* **2007**, *23*, 267–276.
(17) Pieper, R. J.; Ekin, A.; Webster, D. C.; Casse, F.; Callow, J. A.; Callow, M. E. *J. Coat. Technol. Res.* **2007**, *4* (4), 453–461.
(18) Chaudhury, M. K.; Finlay, J. A.; Chung, J. Y.; Callow, M. E.; Callow, J. A. *Biofouling* **2005**, *21*, 41–48.
(19) Tang, Y.; Finlay, J. A.; Kowalke, G. L.; Meyer, A. E.; Bright, F. V.; Callow, M. E.; Callow, J. A.; Wendt, D. E.; Detty, M. R. *Biofouling* **2005**, *21*, 59–71.
(20) Krishnan, S.; Ayothi, R.; Hexemer, A.; Finlay, J. A.; Sohn, K. E.; Perry, R.; Ober, C. K.; Kramer, E. J.; Callow, M. E.; Callow, J. A.; Fischer, D. A. *Langmuir* **2006**, *22*, 5075–5086.
(21) Statz, A.; Finlay, J.; Dalsin, J.; Callow, M.; Callow, J. A.; Merrersmith, P. B. *Biofouling* **2006**, *22*, 391–7399.
(22) Ekin, A.; Webster, D. C. *J. Polym. Sci., Part A: Polym. Chem.* **2006**, *44*, 4880–4894.
(23) Callow, M. E.; Callow, J. A.; Pickett-Heaps, J. D.; Wetherbee, R. *J. Phycol.* **1997**, *33*, 938–947.
(24) Starr, R. C.; Zeikus, J. A. *J. Phycol.* **1987**, *23*, S1–S27.
(25) Finlay, J. A.; Callow, M. E.; Schultz, M. P.; Swain, G. W.; Callow, J. A. *Biofouling* **2002b**, *18*, 251–256.
(26) Figueiredo, M. A. T.; Jain, A. K. Unsupervised learning of finite mixture models. *IEEE Transactions on Pattern Analysis and Machine Intelligence I.*; IEEE: New York, 2002; Vol. 24, pp 381−396.
(27) Gonzalez, R. C.; Woods, R. E. *Digital Image Processing*; Addison-Wesley Longman Publishing Co., Inc.: Boston, MA, 2001
(28) Dempster, A.; Laird, N. M.; Rubin, D. B. *J. R. Stat. Soc., Ser. B* **1977**, *39*, 1–38.
(29) Duda R., H. P.E.; S. D.G. *Pattern Classification*; John Wiley and Sons, Inc.: New York, 2001.
(30) Hartley, R. I.; Zisserman, A. *Multiple View Geometry in Computer Vision*; Cambridge University Press: Cambridge, U. K., 2000; ISBN 0521623049.
(31) Webster, D. C. *JCT Coat. Technol.* **2005**, *2*, 24–29.
(32) Kim, J.; Chisholm, B. J.; Bahr, J. *Biofouling* **2007**, *23*, 113–120.
(33) Rittschof, D.; Orihuela, B.; Stafslien, S.; Daniels, J.; Chisholm, B.; Christianson, D.; Holm, E. *Biofouling* **2008**, *24*, 1–9.

CC800047S